Electronic Supplementary Material (ESI) for Chemical Society Reviews.

Supporting Information

for

The analysis of solution self-assembled polymeric nanomaterials

Joseph P. Patterson, Mathew P. Robin, Christophe Chassenieux, Olivier Colombani and Rachel K. O'Reilly

DOSY NMR

DOSY NMR has also been used for the analysis of polymer and nanoparticles sizes.[1-5] This method essentially measures the self-diffusion coefficient of a magnetic spin in solution. Analogous to DLS, a hydrodynamic radius can then be determined using the Stokes-Einstein equation. Further recent work by Bakkour and co-workers has demonstrated the application of DOSY to the determination of cmc through the examination of diffusion coefficient of a polymer sample across a series of concentrations.[1] At a critical point in the dilution series the diffusion constant will increase significantly as the polymer goes from a self-assembled state to a unimer state and this point has been defined as the cmc. Whilst this method is useful as it measures the property of the assembled structure directly rather than relating the properties of an encapsulate to concentration (as is often done using pyrene),[6] it is somewhat limited in its utility for assemblies with low cmcs given the detection limit of the method. The major benefit of DOSY NMR over other techniques for determining size is that the size can be directly related to a specific chemical species by correlation with its proton spectrum. This could be extremely useful for measuring the encapsulation of small molecules into self-assembled structures or distinguishing between different sized particles in solution.

Zeta Potential

The surface charge of polymeric nanoparticles can be quantified using zeta potential measurements. This is typically achieved through electrophoretic light scattering, and this type of analysis has recently been reviewed for nanoparticles in general.[7]

Nanoparticle Tracking (NTA)

Nanoparticle tracking analysis (NTA) equipment captures the dynamic motion of nanoparticle solutions. Light scattered by the individual nanoparticles upon laser irradiation is detected by a charge-coupled device (CCD) camera, and tracked across the two-dimensional field of view by software to give mean displacements. Corresponding particle diameters can then be calculated using the (two-dimensional) Stokes-Einstein equation, assuming Brownian motion. Size distributions are then simply built up by summation of particles (and their diameters) detected over a certain time period. The lower limit for detectable particle size depends on the ability to detect light scattered by the particles, while the upper limit is affected by the ability to detect the slow diffusion of large particles, as well as the significance of sedimentation for dense particles, and excessive scattering. For polymer nanoparticles this gives a detectable size range of approximately D_{av} = 50-1000 nm.

A major advantage of NTA over DLS is the ability to more accurately resolve multiple size populations, which has been critically evaluated by Jiskoot and co-workers.[8] Using NTA they clearly resolved binary mixtures of polystyrene beads with D_{av} = 60, 100, 200, 400 or 1000 nm (Figure S1A). NTA was also reasonably successful in quantifying the ratio of components in mixtures of 100 and 400nm beads from 3:1 up to 300:1. In both these tests NTA outperformed DLS, which generally requires an order of magnitude difference in D_{av} to resolve multiple populations. Jiskoot *et al.* also showed that because NTA counts individual particles, when a sample contains a minor population with a much larger diameter (*e.g.* aggregated particles or dust), the relative amount of this minor population will be more accurately represented that in conventional light scattering. In contrast, in DLS scattered light intensity will be dominated by this species such that the fast mode (*i.e*. small particles) may not be detected.

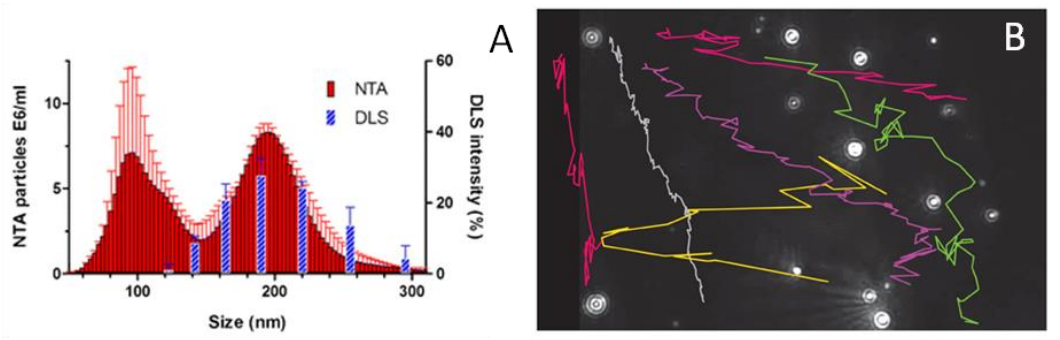

Figure S1: A) Size distribution from NTA and DLS measurements of a mixture of 100 nm and 200 nm diameter polystyrene beads;[8] B) NTA video frame with tracked trajectories of autonomously moving platinum-filled stomatocytes.[9]

NTA has also been used to visualise particles undergoing non-Brownian motion, for example van Hest and co-workers (Figure S1B) imaged the autonomous movement of Pt-loaded polymer stomatocytes driven by catalytic decomposition of hydrogen peroxide fuel using NTA methods.[9]

Currently the most significant limitation for NTA is the requirement that solution concentrations do nt exceed 10^9 particles/mL. This translates to a concentration of *ca.* 10^{-6} g/L for polymeric particles, which is potentially far below values for cmc.

Isotopic substitution/ Deuterium labeling in SANS

The significant difference in SANS observed between hydrogen and deuterium containing materials can be exploited to aid modeling of the data, revealing a wealth of information about the sample. An excellent example of this technique comes from Pedersen et al.[10] They studied polystyrene-b-polyisoprene with a deuterated polystyrene block (*d*-PS-PI), which forms micelles in di-*n*-butyl phthalate (DBP), a slightly selective solvent for PS. SANS measurements were performed in mixtures of deuterated and protonated DBP (*d*-DBP and *p*-DBP respectively), as well as a SAXS measurement in fully protonated DBP.

When the solvent was primarily *p*-DBP, SANS was dominated by scattering from the *d*-PS shell, as this block had the greatest contrast with the surrounding solvent. Conversely, with high *d*-DBP content, SANS was dominated by scattering from the PI core. This can be seen in

Figure S2, where the low *q* peak becomes less pronounced as *d*-DBP increases, due to a decrease in contrast (and hence scattering contribution) from the *d*-PS corona. As PI contrast is much greater than PS contrast in SAXS, the SAXS data is most similar to the highest *d*-DBP SANS data.

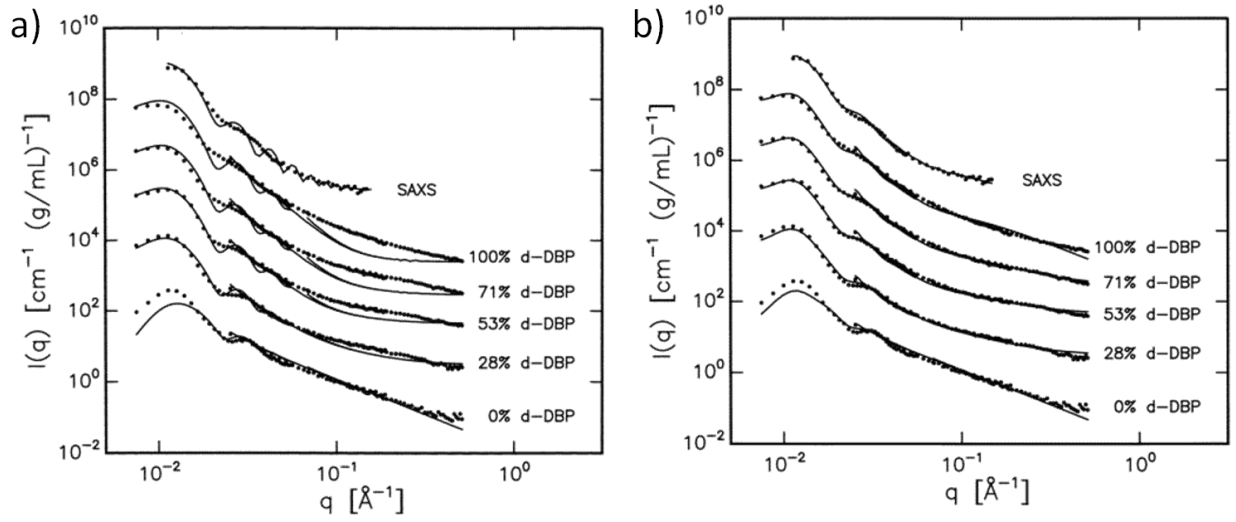

Figure S2. SAXS and SAXS data (•) for d-PS-PI micelles in varying compositions of p and d-DBP, with model (line) for a) monodisperse micelles with a spherical core without concentration fluctuations and b) polydisperse micelles with cylindrical cores with concentration fluctuations.

Simultaneous fitting of the five SANS and one SAXS data sets to one structural model for a micelle with a spherical core (Figure S2a) was unsatisfactory. The main discrepancy between model and data was at low q values, particularly at 100 % d-DBP, indicating that the PI core was poorly modeled. The most satisfactory fit was obtained by a model for a micelle with a partially solvated cylindrical PI core surrounded by solvated Gaussian PS chains (Figure S2b). With this fit values for aggregation number, R_g, core radius and length, volume fraction of solvent in the core, and the surface area available for each PS chain could all be calculated.

General errors associated with scattering experiments

Static Light Scattering: The relative error in the scattering intensity is roughly 1% when the setup (laser and goniometer) is perfectly aligned. The major contribution to the relative error on the weight average molecular weight of the scattering particles mostly arises from the error in specific refractive index increment. A 5% relative error bar is generally accepted for *dn/dC*

leading to a relative error bar of 10% on M_w. The relative error in the radius of gyration is around 5% provided the experimental setup is well aligned, that the measurements are run in the Guinier regime, and lastly that R_g is larger than 20 nm and smaller than 80 nm when measured with a conventional LS setup.

Dynamic Light Scattering: The relative error bar on the hydrodynamic radius is generally 5% provided the baseline is properly measured – that is to say that the duration of the experiments is long enough for achieving good statistics for the data.[11]

SAXS and SANS: The standard deviations in the parameters derived from these techniques must account for the resolution of the spectrometer used for the experiments. This is quite poor for SANS. Habits regarding the resolution function vary considerably from one group to another. Some just never mention the resolution and include polydispersity in the object size without further ado,[12] some simply mention that resolution has been taken into account in the analysis of the scattering data,[13] and finally some thoroughly describe the computational methods used to include both polydispersity and resolution in their data fitting.[14] In all cases, the reduction of the data must be properly carried out, as outlined in a recent review.[15]

ESEM

It is also possible to image samples in the liquid phase through the use of Environmental SEM (ESEM),[16] however, there have been no examples for polymer assemblies, possibly due to the reduced resolution and to the requirement that the samples be surface active.

Additional suggested reading

Amphiphilic block copolymers

I.W.Hamley, *Block copolymers in solution: Fundamentals and Applications,* Wiley, 2005

DLS

Useful info from nanocomposix

http://nanocomposix.com/sites/default/files/handbooks/introduction.pdf

http://nanocomposix.com/sites/default/files/nanoComposix%20Guidelines%20for%20DLS%20Measurements%20and%20Analysis.pdf

DLS and SLS

Paper describing the light scattering of the Tabaco Mosaic Virus (cylindrical nanoparticle). Particularly good for information of light scattering for non-spherical particles.

N. C. Santos and M. A. Castanho, *Biophys. J.*, 1996, **71**, 1641-1650

For many examples of different experimental set-ups and data analysis appropriate for different samples (Chapter 5).

W. Schärtl, *Light scattering from polymer solutions and nanoparticle dispersions*, Springer Berlin, 2007.

For more information on the CONTIN

S. W. Provencher, J. Hendrix, M. L. De and N. Paulussen, *J. Chem. Phys.*, 1978, **69**, 4273-4276

SANS and SAXS

A general review

I. W. Hamley and V. Castelletto, *Prog. Polym. Sci.*, 2004, **29**, 909-948

A review on small angle scattering data analysis and reduction

J. S. Pedersen. Adv. Coll. Inerface. Sci. **70**, 171-210

The NIST Scattering length density (SLD) calculator

http://www.ncnr.nist.gov/resources/sldcalc.html

A review focussing on stopped-flow experiments

I. Grillo, *Curr. Opin. Colloid In.*, 2009, **14**, 402-408.

TEM

Extremely useful JAVA application from the University of Liverpool explaining how TEM works

http://www.matter.org.uk/tem/

Although a very technical book, the definitive guide is D. B. Williams and C. B. Carter, *The Transmission Electron Microscope*, Springer, 1996.

Cryo-TEM

S. Zhong and D. J. Pochan, *Polym. Rev.*, 2010, **50**, 287-320

H. Cui, T. K. Hodgdon, E. W. Kaler, L. Abezgauz, D. Danino, Maya Lubovsky, Y. Talmond and D. J. Pochan, *Soft Matter*, 2007,**3**, 945-955

C. J. Newcomb, T. J. Moyer, S. S. Lee and S. I. Stupp, *Curr. Opin. Colloid. In.*, 2012, **17**, 350-359

References

1. Y. Bakkour, V. Darcos, S. Li and J. Coudane, *Polym. Chem.*, 2012, **3**, 2006-2010.
2. P. S. Denkova, L. L. Van, I. Verbruggen and R. Willem, *J. Phys. Chem. B*, 2008, **112**, 10935-10941.
3. W. Li, H. Chung, C. Daeffler, J. A. Johnson and R. H. Grubbs, *Macromolecules (Washington, DC, U. S.)*, 2012, **45**, 9595-9603.
4. G. Canzi, A. A. Mrse and C. P. Kubiak, *J. Phys. Chem. C*, 2011, **115**, 7972-7978.
5. R. Mallol, M. A. Rodriguez, M. Heras, M. Vinaixa, N. Plana, L. Masana, G. A. Morris and X. Correig, *Anal. Bioanal. Chem.*, 2012, **402**, 2407-2415.
6. J. Aguiar, P. Carpena, J. A. Molina-Bolivar and R. C. Carnero, *J. Colloid Interface Sci.*, 2003, **258**, 116-122.
7. T. L. Doane, C.-H. Chuang, R. J. Hill and C. Burda, *Acc. Chem. Res.*, 2011, **45**, 317-326.
8. V. Filipe, A. Hawe and W. Jiskoot, *Pharm. Res.*, 2010, **27**, 796-810.
9. D. A. Wilson, R. J. M. Nolte and J. C. M. van Hest, *Nat. Chem.*, 2012, **4**, 268-274.
10. J. S. Pedersen, I. W. Hamley, C. Y. Ryu and T. P. Lodge, *Macromolecules*, 2000, **33**, 542-550.
11. H. Ruf, *Biophys. J.*, 1989, **56**, 67-78.
12. J.-F. Berret, P. Hervé, O. Aguerre-Chariol and J. Oberdisse, *The Journal of Physical Chemistry B*, 2003, **107**, 8111-8118.
13. I. Goldmints, G.-e. Yu, C. Booth, K. A. Smith and T. A. Hatton, *Langmuir*, 1999, **15**, 1651-1656.
14. S. Okabe, S. Sugihara, S. Aoshima and M. Shibayama, *Macromolecules*, 2002, **35**, 8139-8146.

15. A. Brulet, D. Lairez, A. Lapp and J.-P. Cotton, *J. Appl. Crystallogr.*, 2007, **40**, 165-177.
16. D. J. Stokes, *Philosophical Transactions: Mathematical, Physical and Engineering Sciences*, 2003, **361**, 2771-2787.